JOURNAL OF VIROLOGY, Sept. 2008, p. 8882–8886 Vol. 82, No. 17
0022-538X/08/$08.00+0 doi:10.1128/JVI.00920-08

NOTES

Experimental Optic Neuritis Induced by a Demyelinating Strain of Mouse Hepatitis Virus▽

Kenneth S. Shindler,[1] Lawrence C. Kenyon,[2] Mahasweta Dutt,[1] Susan T. Hingley,[3] and Jayasri Das Sarma[4]*

University of Pennsylvania, Scheie Eye Institute and FM Kirby Center for Molecular Ophthalmology, Philadelphia, Pennsylvania 19104[1]; Department of Pathology, Anatomy and Cell Biology, Thomas Jefferson University, Philadelphia, Pennsylvania 19107[2]; Philadelphia College of Osteopathic Medicine, Philadelphia, Pennsylvania 19131[3]; and Department of Neurology, Thomas Jefferson University, Philadelphia, Pennsylvania 19107[4]

Received 2 May 2008/Accepted 18 June 2008

Optic neuritis (ON), an inflammatory demyelinating optic nerve disease, occurs in multiple sclerosis (MS). Pathological mechanisms and potential treatments for ON have been studied via experimental autoimmune MS models. However, evidence suggests that virus-induced inflammation is a likely etiology triggering MS and ON; experimental virus-induced ON models are therefore required. We demonstrate that MHV-A59, a mouse hepatitis virus (MHV) strain that causes brain and spinal cord inflammation and demyelination, induces ON by promoting mixed inflammatory cell infiltration. In contrast, MHV-2, a nondemyelinating MHV strain, does not induce ON. Results reveal a reproducible virus-induced ON model important for the evaluation of novel therapies.

Significant neuronal damage, with loss of retinal ganglion cell (RGC) axons that comprise the optic nerve, occurs following inflammatory optic neuritis (ON) and correlates with permanent vision loss (2, 6, 28). Experimental ON is a useful model to examine mechanisms of neuronal damage in multiple sclerosis (MS) because RGCs can readily be labeled and quantified (23). Rodents immunized with myelin proteins develop experimental autoimmune encephalomyelitis (EAE), a model of MS with inflammation in the brain, spinal cord, and optic nerves (12). Mechanisms of neuronal damage during ON in EAE have been examined but vary between chronic (16, 19) and relapsing (23) EAE models, suggesting that different causes of ON may mediate vision-threatening neuronal damage by distinct mechanisms.

MS may be caused by a viral infection triggering an immune response against myelin (1, 26). Studies of virus-mediated models of MS are therefore important for our understanding of disease mechanisms and the development of novel therapies. While virus-induced models of MS exist (15, 26), the incidence of ON has not been characterized.

Mouse hepatitis virus (MHV) infection in mice has been used as a model for virus-induced demyelination that mimics many pathological features of MS (9, 13, 15, 27, 29). Some neurotropic strains of MHV induce a biphasic neurological disease with acute meningoencephalitis, followed by chronic demyelination (15). Similarly to results for autoimmune models of MS, Dandekar et al. recently demonstrated that axonal damage occurs in mice with MHV-induced demyelination (3). It is not known whether the inflammatory demyelination and axonal loss observed to occur in the MHV-infected mouse brain and spinal cord also affect the optic nerve.

In the current study, we inoculated mice with plaque-purified demyelinating strain MHV-A59 (14, 15) and nondemyelinating strain MHV-2 (10). MHV-A59 infects a variety of cell types, including neurons, astrocytes, oligodendrocytes, microglia, and ependymal cells (11, 13, 15, 30), in the central nervous system (CNS) and causes acute encephalitis, meningitis, hepatitis, and chronic demyelination. In contrast, MHV-2, a strain closely related to MHV-A59, has a limited ability to invade the brain and spinal cord, causing meningitis without encephalitis or demyelination (4, 20), making it an appropriate experimental negative control for our understanding of the mechanisms of MHV-A59-induced CNS inflammatory disease processes.

MHV-A59 and MHV-2 were propagated and assayed as described previously (20). Four-week-old, virus-free, C57BL/6 mice (Jackson Laboratory) were inoculated intracranially with 50% lethal doses of MHV-A59 (2,000 PFU) or MHV-2 (50 PFU), as described previously (20), and monitored daily for mortality and signs of disease (15, 20). Mice were sacrificed 3, 5, 7, 15, or 30 days postinoculation and perfused with phosphate-buffered saline followed by phosphate-buffered saline containing 4% paraformaldehyde. Liver, brain, spinal cord, and optic nerve tissues were collected, postfixed in 4% paraformaldehyde overnight at room temperature, and embedded in paraffin. To confirm expected virulence, livers were cut in 5-μm sections and stained with hematoxylin and eosin (H&E), and pathology of moderate to severe hepatitis was characterized by multiple foci of necrosis (data not shown), similarly to

* Corresponding author. Mailing address: 302 JHN, 900 Walnut Street, Department of Neurology, Thomas Jefferson University, Philadelphia, PA 19107. Phone: (215) 955-9412. Fax: (215) 503-5848. E-mail: Jayasri.Das-Sarma@jefferson.edu.

▽ Published ahead of print on 25 June 2008.

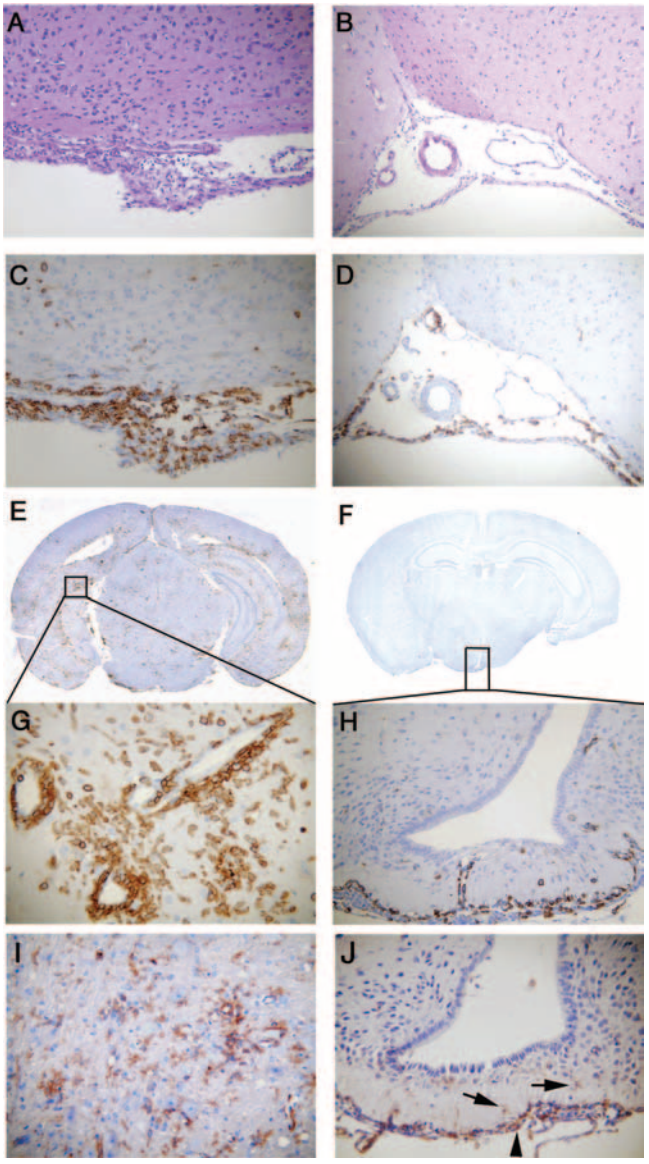

FIG. 1. Histopathology of brain sections during acute infection with MHV-A59 compared to MHV-2. Serial coronal sections (5 μm thick) from MHV-A59- and MHV-2-infected mice at day 5 postinoculation were stained with H&E (A and B) or immunostained for LCA (C to H) or CD11b (I and J). Histopathology shows acute meningitis characterized by brisk leptomeningeal inflammatory infiltration in the subarachnoid space of the basal forebrain in both MHV-A59-infected (A and C) and MHV-2-infected (B and D) mice. Coronal sections stained for LCA show acute encephalitis in the MHV-A59-infected mouse brain, characterized by the presence of inflammatory infiltrates throughout the parenchyma (E) and the formation of perivascular cuffing (G) at high magnification, whereas in MHV-2 infection, infiltrating inflammatory cells were rarely observed in brain parenchyma (F) and, when present, were restricted to the subependyma (H). The majority of LCA-positive inflammatory cells stained positive for the macrophage/microglia marker CD11b in MHV-A59-infected brain parenchyma (I), and the few positive cells in the MHV-2-infected brain (J) remained restricted to the subependyma (arrows). Original magnifications are ×100 for panels A to D and H and ×200 for panels G, I, and J. Panels E and F are laser-scanned images.

methods from prior studies (17, 20). Experiments were repeated three times with three to five mice in each group.

To characterize virus-induced inflammation in the brain, 5-μm coronal sections were stained with H&E. Both MHV-A59 and MHV-2 induced meningitis (Fig. 1A and B), similarly to findings from prior studies (20), although the type of inflammatory cells present was not fully characterized previously. Serial sections were therefore stained for immunohistochemical analysis by the avidin-biotin-immunoperoxidase technique (Vector Laboratories, Burlington, CA) using 3,3′-diaminobenzidine as the substrate and a 1:100 dilution of anti-CD45 (leukocyte common antigen [LCA] LY-5; BD Pharmingen), anti-CD11b (OX42; Santa Cruz Biotechnology), or anti-CD3 (PC3/188A; Santa Cruz) as the primary immunoglobulin G antibody. LCA staining confirmed that the increased numbers of cells in the meninges of the MHV-A59- or MHV-2-infected CNS consist predominantly of infiltrating inflammatory cells (Fig. 1C and D). Similarly to results from prior studies (20), MHV-A59 also induced focal acute encephalitis, characterized by inflammatory infiltrates in brain parenchyma with perivascular cuffing (Fig. 1E and G), whereas in the MHV-2-infected brain, inflammatory cells were restricted to the meninges, choroid plexus, and subependymal region, with minimal, if any, invasion of brain parenchyma (Fig. 1F and H). The majority of infiltrating cells were $CD11b^+$, a macrophage/microglia marker (Fig. 1I and J). Some CD3-stained infiltrating T cells were also found (data not shown), although nonspecific background staining of neurons with available anti-CD3 antibodies made staining difficult to quantify. Together, these data suggest that MHV-induced CNS inflammation consists of mixed inflammatory cells, predominantly macrophages/microglia. Viral antigen was stained (5), and the presence of MHV-A59 antigen in the brain was confirmed, as in prior studies (data not shown).

Pathology was also assessed in five to seven cross-sections of spinal cord from cervical, thoracic, and lumbar regions. Similarly to results for the brain, H&E and LCA staining demonstrated that both MHV-A59 and MHV-2 induced meningitis (data not shown), whereas only MHV-A59 induced myelitis (Fig. 2A and C). In MHV-2 infection, inflammatory cells were rare and restricted to an area near the ependymal cell lining of the central canal (Fig. 2B and D). Similarly to results for the brain, the majority of inflammatory cells were $CD11b^+$ (data not shown). Luxol fast blue (LFB) staining (20) was performed to visualize myelin. Demyelinating plaques developed as early as day 5 postinoculation in MHV-A59-infected mice (Fig. 2E), with no demyelination in MHV-2-infected mice (Fig. 2F). Demyelinating plaques were quantified on a 0-to-3 scale in four quadrants from two spinal cord levels for each mouse; thus, approximately 100 total quadrants were examined for each virus over three experiments. Day 30 postinoculation tissue sections from MHV-A59-infected mice showed a pattern of demyelination similar to that on day 5, but the number and area of plaques were larger (Fig. 2G), and MHV-2-infected mice did not exhibit any demyelination. To avoid a high mortality rate of MHV-2 due to hepatitis, we used 50% lethal doses (50 PFU). However, to ensure that the inability of MHV-2 to cause encephalitis or demyelination is not dose dependent, we also inoculated mice with MHV-A59 at 50 PFU. MHV-A59 produced larger demyelinating lesions when given at 2,000 PFU than at 50 PFU, but with both doses, 100%

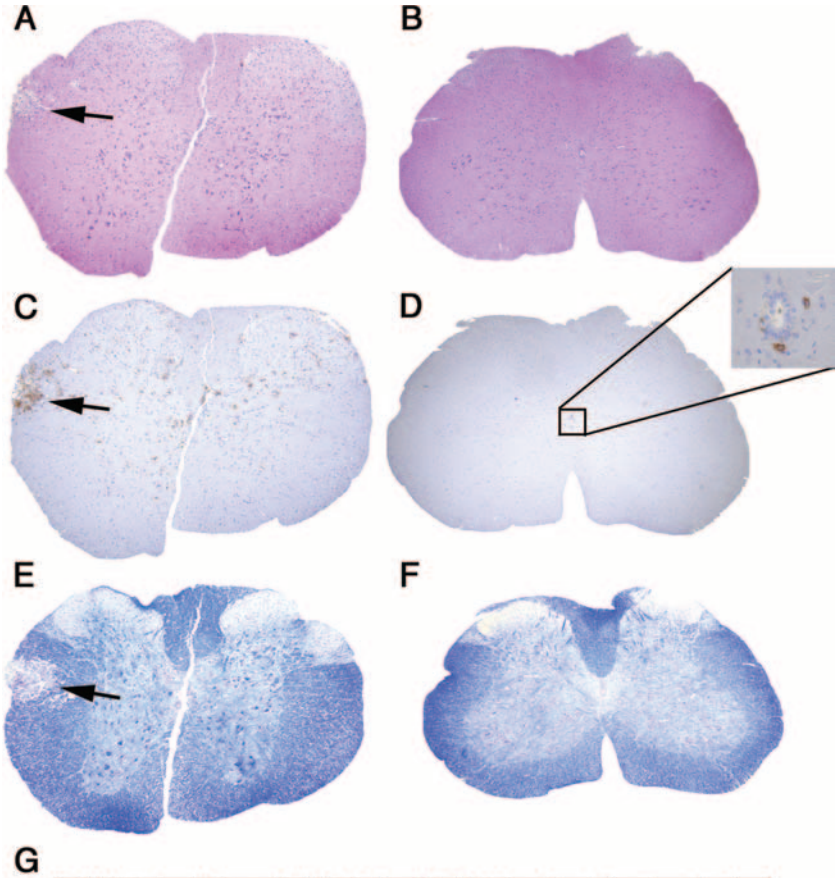

MHV strain	Days of post-infection	% of mice with demyelination	% of quadrants positive for demyelination	Severity of demyelination (score)
MHV-A59	5	100	30	1.41 ± 0.148
	30	100	60	2.38 ± 0.128
MHV-2	5	0	0	0
	30	0	0	0

FIG. 2. Comparative histopathology of MHV-A59- and MHV-2-infected mouse spinal cords. Serial cross sections (5 μm thick) from MHV-A59- and MHV-2-infected mouse spinal cords at day 5 postinoculation were stained with H&E (A and B), LCA (C and D), or LFB (E and F). Several inflammatory lesions (A), with infiltrating LCA-positive cells (C), were observed in the MHV-A59-infected mouse spinal cord (arrows indicate lesion area), whereas in the MHV-2-infected mouse spinal cord no parenchymal lesions were observed (B), with only rare LCA-positive infiltrates observed near the central canal (D). An adjacent section of an MHV-A59-infected spinal cord shows a loss of myelin by LFB staining (E) (arrow indicates demyelinated area), whereas normal myelin was observed in an MHV-2-infected mouse spinal cord (F). Original magnification, ×40. (G) Quantification of demyelinated plaques identified in day 5 and day 30 spinal cords. Four quadrants were scored at two separate levels in each spinal cord, and the percentages of mice and percentages of quadrants observed to contain demyelinated plaques are shown. Cumulative data representing three experiments, with three to five mice/group in each experiment, are shown. Mean (±standard error of the mean) severity of demyelination is scored on a four-point scale (0, none; 1, rare foci; 2, a few areas of demyelination; 3, large [confluent] areas of demyelination).

of mice were affected. Our results confirm earlier findings that MHV-A59 induces demyelination whereas MHV-2 is non-demyelinating at day 30 (20). Demyelination was not previously assessed at earlier time points. Here we demonstrate that demyelination begins as early as day 5 postinoculation, indicating that MHV-A59-induced myelin damage begins at the time of acute inflammation, similarly to what is observed for MS and EAE lesions (12).

The presence of LCA-positive inflammation and associated demyelination in the brain and spinal cord led us to hypothesize that MHV-A59-infected mice may develop ON similar to experimental ON in mice with EAE. Optic nerves from MHV-A59- and MHV-2-infected mice were cut into 5-μm longitudinal sections and stained with H&E and inflammatory cell markers. For comparison, relapsing EAE was induced in 8-week-old SJL/J mice by immunization with proteolipid protein peptide, as described previously (23). Mice were sacrificed on day 11 postimmunization, when there were incidences of ON peaks (23), and optic nerves were isolated. Inflammatory cells infiltrating the optic nerve sheath and parenchyma are shown by H&E and LCA staining (Fig. 3A and B) 5 days after inoculation with MHV-A59, with results similar to inflamma-

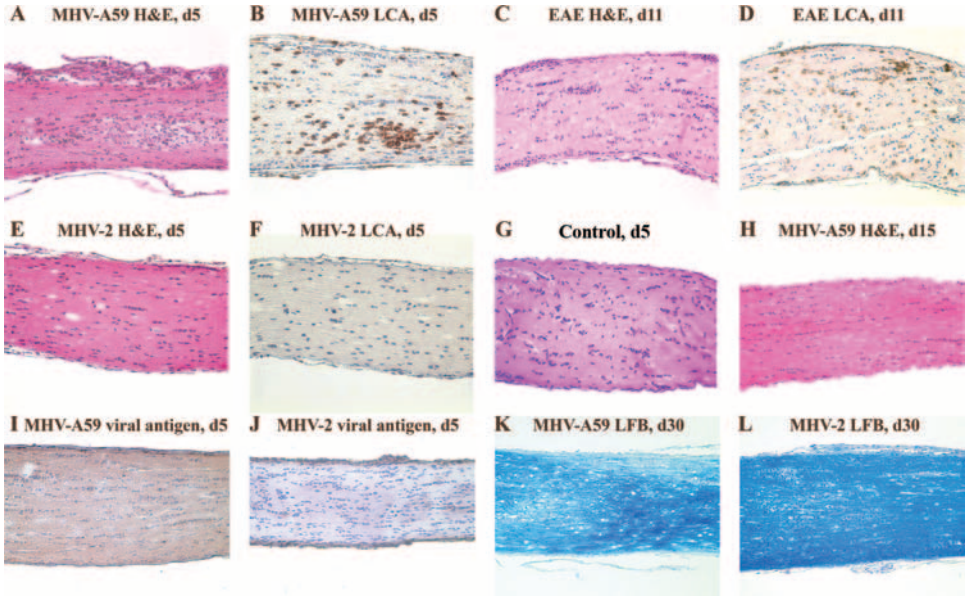

FIG. 3. Optic nerve histopathology from MHV-A59-infected mice, MHV-2-infected mice, and mice with EAE. Longitudinal sections (5 μm thick) of optic nerves from MHV-infected mice and mice with EAE are shown. Numerous inflammatory cells are evident in an MHV-A59-infected optic nerve with ON 5 days (d5) postinoculation stained by H&E (A) and LCA (B). Similar inflammation is seen in the EAE optic nerve 11 days postimmunization (C and D). The optic nerve 5 days after inoculation with MHV-2 (E) shows a lack of inflammation, with no LCA staining detected (F), similar to the histology of a normal, control optic nerve (G). MHV-A59-induced inflammation resolves by day 15 postinoculation (H). Viral antigen staining of an optic nerve from an MHV-A59-infected mouse shows low-level axonal staining (I), whereas no viral antigen is detected in an MHV-2-infected mouse optic nerve (J). LFB staining 30 days postinoculation demonstrates a loss of myelin in a mouse with MHV-A59 ON (K) and normal myelin staining in an MHV-2-infected mouse (L). Original magnification, ×20.

tion seen for EAE ON (Fig. 3C and D). In contrast, optic nerves from MHV-2-infected mice did not develop ON (Fig. 3E and F) and had a histological appearance similar to that of control optic nerves (Fig. 3G). Both $CD11b^+$ and fewer $CD3^+$ cells were noted in MHV-A59-infected optic nerves, similarly to results for the brain; however, background staining levels for these and control nerves made the results difficult to interpret (data not shown), and as better antibodies become available, further evaluation will be needed to confirm these observations. By day 15 after MHV-A59 infection, optic nerve inflammation completely resolved (Fig. 3H).

Detection of viral antigen in optic nerves was limited to axons, because there are no neuronal cell bodies present. Light diffuse staining detected in optic nerves from MHV-A59-infected mice (Fig. 3I) but not MHV-2-infected mice (Fig. 3J) suggests that the MHV-A59 viral antigen is likely present in optic nerve axons. Consistent with the observed pattern of inflammation, optic nerves from MHV-A59-infected mice had areas of demyelination detected by LFB staining 30 days postinoculation (Fig. 3K), whereas no demyelination occurred in MHV-2-infected mice (Fig. 3L).

The degree of optic nerve inflammation was scored on a

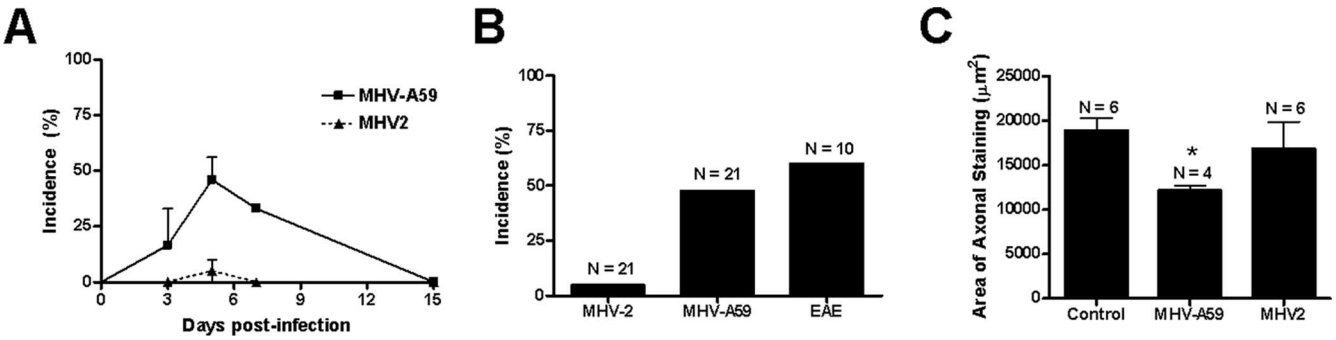

FIG. 4. Incidence of ON and axonal loss in MHV-infected mice and mice with EAE. (A) ON, determined by the presence of any level of inflammation in the optic nerve, is detected as early as day 3 after inoculation with MHV-A59. The incidence increases by day 5, persists at day 7, and resolves by day 15. In contrast, almost no MHV-2-infected mice develop ON over the same time course. The mean (±standard error of the mean) incidence from three experiments is shown. (B) The peak incidence of MHV-A59-induced ON, detected at day 5 postinoculation, is 48% (10 of 21 nerves), whereas only 1 of 21 nerves from MHV-2-infected mice developed ON. Sixty percent (6 of 10) of optic nerves from mice with EAE developed ON at the peak of inflammation on day 11 postimmunization. (C) The area of axonal staining (mean ± standard error of the mean) detected by Bielschowsky silver impregnation is significantly lower in optic nerves from MHV-A59-infected mice than in optic nerves from control, uninfected mice or MHV-2-infected mice (*, $P \leq 0.05$).

0-point (no inflammation) to 4-point (severe inflammation) scale described previously (22–24), with any amount of inflammation (score of 1 to 4) considered positive for ON. ON was detected as early as 3 days after inoculation with MHV-A59, with the peak incidence at day 5 and resolution by day 15 (Fig. 4A). At the peak of ON (day 5), almost 50% (10 of 21) of optic nerves examined from MHV-A59-infected mice had ON (Fig. 4B), with an average relative inflammation score of 1.7 ± 0.21, whereas only 1 of 21 nerves from MHV-2-infected mice had even mild inflammation (score of 1.0). The incidence of ON in mice with EAE was 60% (6 of 10), with a 1.83 ± 0.31 average inflammation score, similar to results from prior studies (23, 24) and comparable to the incidence induced by MHV-A59 infection. To examine whether MHV-A59-induced ON also leads to axonal loss, optic nerves were stained by Bielschowsky silver impregnation, and the area of axonal staining was quantified as described previously (25). Thirty days postinoculation, nerves from MHV-A59-infected mice showed significantly decreased axonal staining compared to control nerves or nerves from MHV-2-infected mice (Fig. 4C).

Our results demonstrate that MHV-A59, but not MHV-2, induces demyelination in the CNS during acute encephalitis as early as 5 days postinoculation, in addition to the chronic demyelination previously observed to occur at day 30 (20). We demonstrated that inflammation triggered by MHV infection consists of mixed inflammatory cells, predominantly macrophages/microglia, which differs somewhat from autoimmune models of MS, where infiltrating T cells are significant contributors to pathology (12, 18). Importantly, MHV-A59 also induces ON with similar levels of severity and incidence, as seen in the autoimmune antigen-triggered EAE model. Experimental ON is an important model being used to characterize neuronal damage and develop novel therapies for MS (7, 19, 21, 24), but studies have shown that different EAE models, induced by distinct antigens, lead to different mechanisms of RGC loss (8, 23). The MHV-A59-induced ON model will provide a critical adjunct to study the pathophysiology of ON secondary to virus-mediated inflammation, as this is one mechanism that can cause ON and MS in human patients.

This work was supported by FG 1431-A-1 and RG3774A2-1 from the National Multiple Sclerosis Society and the M. E. Groff Surgical Medical Research and Education Charitable Trust (F76401) to J.D.S. and by NIH grant EY015098, a career development award from Research to Prevent Blindness, and unrestricted funding from the Paul and Evanina Mackall Foundation Trust and the F. M. Kirby Foundation to K.S.S.

We thank Elsa Aglow and Rhonda Walters for histological assistance and Kevin Kralik for technical assistance.

REFERENCES

1. **Allen, I., and B. Brankin.** 1993. Pathogenesis of multiple sclerosis—the immune diathesis and the role of viruses. J. Neuropathol. Exp. Neurol. **52:**95–105.
2. **Costello, F., S. Coupland, W. Hodge, G. R. Lorello, J. Koroluk, Y. I. Pan, M. S. Freedman, D. H. Zackon, and R. H. Kardon.** 2006. Quantifying axonal loss after optic neuritis with optical coherence tomography. Ann. Neurol. **59:**963–969.
3. **Dandekar, A. A., G. F. Wu, L. Pewe, and S. Perlman.** 2001. Axonal damage is T cell mediated and occurs concomitantly with demyelination in mice infected with a neurotropic coronavirus. J. Virol. **75:**6115–6120.
4. **Das Sarma, J., L. Fu, S. T. Hingley, M. M. Lai, and E. Lavi.** 2001. Sequence analysis of the S gene of recombinant MHV-2/A59 coronaviruses reveals three candidate mutations associated with demyelination and hepatitis. J. Neurovirol. **7:**432–436.
5. **Das Sarma, J., K. Iacono, L. Gard, R. Marek, L. C. Kenyon, M. Koval, and S. R. Weiss.** 2008. Demyelinating and nondemyelinating strains of mouse hepatitis virus differ in their neural cell tropism. J. Virol. **82:**5519–5526.
6. **Fisher, J. B., D. A. Jacobs, C. E. Markowitz, S. L. Galetta, N. J. Volpe, M. L. Nano-Schiavi, M. L. Baier, E. M. Frohman, H. Winslow, T. C. Frohman, P. A. Calabresi, M. G. Maguire, G. R. Cutter, and L. J. Balcer.** 2006. Relation of visual function to retinal nerve fiber layer thickness in multiple sclerosis. Ophthalmology **113:**324–332.
7. **Guyton, M. K., E. A. Sribnick, S. K. Ray, and N. L. Banik.** 2005. A role for calpain in optic neuritis. Ann. N. Y. Acad. Sci. **1053:**48–54.
8. **Hobom, M., M. K. Storch, R. Weissert, K. Maier, A. Radhakrishnan, B. Kramer, M. Bahr, and R. Diem.** 2004. Mechanisms and time course of neuronal degeneration in experimental autoimmune encephalomyelitis. Brain Pathol. **14:**148–157.
9. **Houtman, J. J., and J. O. Fleming.** 1996. Pathogenesis of mouse hepatitis virus-induced demyelination. J. Neurovirol. **2:**361–376.
10. **Keck, J. G., L. H. Soe, S. Makino, S. A. Stohlman, and M. M. Lai.** 1988. RNA recombination of murine coronaviruses: recombination between fusion-positive mouse hepatitis virus A59 and fusion-negative mouse hepatitis virus 2. J. Virol. **62:**1989–1998.
11. **Knobler, R. L., M. Dubois-Dalcq, M. V. Haspel, A. P. Claysmith, P. W. Lampert, and M. B. Oldstone.** 1981. Selective localization of wild type and mutant mouse hepatitis virus (JHM strain) antigens in CNS tissue by fluorescence, light and electron microscopy. J. Neuroimmunol. **1:**81–92.
12. **Kornek, B., M. K. Storch, R. Weissert, E. Wallstroem, A. Stefferl, T. Olsson, C. Linington, M. Schmidbauer, and H. Lassmann.** 2000. Multiple sclerosis and chronic autoimmune encephalomyelitis: a comparative quantitative study of axonal injury in active, inactive, and remyelinated lesions. Am. J. Pathol. **157:**267–276.
13. **Lavi, E., P. S. Fishman, M. K. Highkin, and S. R. Weiss.** 1988. Limbic encephalitis after inhalation of a murine coronavirus. Lab. Investig. **58:**31–36.
14. **Lavi, E., D. H. Gilden, M. K. Highkin, and S. R. Weiss.** 1984. Persistence of mouse hepatitis virus A59 RNA in a slow virus demyelinating infection in mice as detected by in situ hybridization. J. Virol. **51:**563–566.
15. **Lavi, E., D. H. Gilden, Z. Wroblewska, L. B. Rorke, and S. R. Weiss.** 1984. Experimental demyelination produced by the A59 strain of mouse hepatitis virus. Neurology **34:**597–603.
16. **Meyer, R., R. Weissert, R. Diem, M. K. Storch, K. L. de Graaf, B. Kramer, and M. Bahr.** 2001. Acute neuronal apoptosis in a rat model of multiple sclerosis. J. Neurosci. **21:**6214–6220.
17. **Navas, S., S. H. Seo, M. M. Chua, J. D. Sarma, E. Lavi, S. T. Hingley, and S. R. Weiss.** 2001. Murine coronavirus spike protein determines the ability of the virus to replicate in the liver and cause hepatitis. J. Virol. **75:**2452–2457.
18. **Noseworthy, J. H., C. Lucchinetti, M. Rodriguez, and B. G. Weinshenker.** 2000. Multiple sclerosis. N. Engl. J. Med. **343:**938–952.
19. **Qi, X., A. S. Lewin, L. Sun, W. W. Hauswirth, and J. Guy.** 2007. Suppression of mitochondrial oxidative stress provides long-term neuroprotection in experimental optic neuritis. Investig. Ophthalmol. Vis. Sci. **48:**681–691.
20. **Sarma, J. D., L. Fu, S. T. Hingley, and E. Lavi.** 2001. Mouse hepatitis virus type-2 infection in mice: an experimental model system of acute meningitis and hepatitis. Exp. Mol. Pathol. **71:**1–12.
21. **Sattler, M. B., D. Merkler, K. Maier, C. Stadelmann, H. Ehrenreich, M. Bahr, and R. Diem.** 2004. Neuroprotective effects and intracellular signaling pathways of erythropoietin in a rat model of multiple sclerosis. Cell Death Differ. **11**(Suppl 2)**:**S181–S192.
22. **Shao, H., Z. Huang, S. L. Sun, H. J. Kaplan, and D. Sun.** 2004. Myelin/oligodendrocyte glycoprotein-specific T-cells induce severe optic neuritis in the C57BL/6 mouse. Investig. Ophthalmol. Vis. Sci. **45:**4060–4065.
23. **Shindler, K. S., Y. Guan, E. Ventura, J. Bennett, and A. Rostami.** 2006. Retinal ganglion cell loss induced by acute optic neuritis in a relapsing model of multiple sclerosis. Mult. Scler. **12:**526–532.
24. **Shindler, K. S., E. Ventura, T. S. Rex, P. Elliott, and A. Rostami.** 2007. SIRT1 activation confers neuroprotection in experimental optic neuritis. Investig. Ophthalmol. Vis. Sci. **48:**3602–3609.
25. **Shindler, K. S., E. Ventura, M. Dutt, and A. Rostami.** 3 June 2008. Inflammatory demyelination induces axonal injury and retinal ganglion cell apoptosis in experimental optic neuritis. Exp. Eye Res. doi:10.1016/j.exer.2008.05.017.
26. **Sospedra, M., and R. Martin.** 2005. Immunology of multiple sclerosis. Annu. Rev. Immunol. **23:**683–747.
27. **Stohlman, S. A., and L. P. Weiner.** 1981. Chronic central nervous system demyelination in mice after JHM virus infection. Neurology **31:**38–44.
28. **Trip, S. A., P. G. Schlottmann, S. J. Jones, D. R. Altmann, D. F. Garway-Heath, A. J. Thompson, G. T. Plant, and D. H. Miller.** 2005. Retinal nerve fiber layer axonal loss and visual dysfunction in optic neuritis. Ann. Neurol. **58:**383–391.
29. **Weiner, L. P.** 1973. Pathogenesis of demyelination induced by a mouse hepatitis. Arch. Neurol. **28:**298–303.
30. **Weiner, L. P., R. T. Johnson, and R. M. Herndon.** 1973. Viral infections and demyelinating diseases. N. Engl. J. Med. **288:**1103–1110.